

# COUPLING HYDROGRAPH SEPARATION AND HIGH-FREQUENCY TURBIDITY DATA TO ASSESS THE SIGNIFICANCE OF RUNOFF AND BASEFLOW IN TURBIDITY GENERATION

**Amirreza Zarnaghsh**, Ph.D. Candidate, Department of Civil, Environmental, and Architectural Engineering, University of Kansas, Lawrence, Kansas, [azarnaghsh@ku.edu](mailto:azarnaghsh@ku.edu)

**Admin Husic**, Assistant Professor, Department of Civil, Environmental, and Architectural Engineering, University of Kansas, Lawrence, Kansas, [ahusic@ku.edu](mailto:ahusic@ku.edu)

## Introduction

Sediment pollution of surface rivers and streams has become a major concern in many parts of the world due to its potential negative consequences including water quality degradation, increasing water treatment costs, and damage to infrastructure (Vercruysse et al., 2017; Oeurng et al., 2010). The majority of sediment delivery to freshwater systems occurs during storm events when the sediment concentrations can increase several orders of magnitude over short time scales (Ziegler et al., 2014; Mukundan et al., 2013). With the advent of high-frequency water quality sensors, many researchers have investigated the asynchronous relationship between discharge and sediment during storm events, termed “hysteresis”, to identify sources and pathways of sediment (Lloyd et al., 2016; Wymore et al., 2019). Hysteresis patterns have a high amount of spatial and temporal variability and are dependent on many factors, including land use and climatic conditions (Zarnaghsh and Husic, 2021). Another challenge in understanding sediment transport dynamics originates from the uncertainty regarding the relative contribution of different water components such as surface runoff and subsurface baseflow to in-stream variations of sediment concentrations. While many researchers have employed hydrograph separation techniques to quantify runoff and baseflow contributions to total streamflow (Hasenmueller et al., 2017; Miller et al., 2017), less is known about how the timing of runoff and baseflow arrival coincides with in-stream sediment generation. Therefore, a better understanding of sediment delivery processes can be obtained by investigating sediment hysteresis patterns and flow pathway influence on fluvial sediment generation across large spatial and temporal scales.

In this study, we analyzed sediment hysteresis for nearly 38,000 storm events in more than 260 basins across the contiguous United States (CONUS) from 2000 to 2022. Discharge and sensor data were retrieved from stream sites monitored by the United States Geological Survey (USGS) and National Ecological Observatory Network (NEON). We conducted hydrograph separation using specific conductance data and coupled these results to the high-frequency turbidity data. Thereafter, we developed a new index –  $\beta'_{runoff}$  – to quantify the relative contribution of surface runoff to turbidity generation during a storm event. We ask: (1) what are the spatial distribution patterns in sediment sediment-discharge, sediment-runoff, and sediment-baseflow relationships during storm events and (2) how do watershed characteristics, such as land use, soil type, topography, and climate influence fluvial sediment responses? We believe such inferences can help watershed managers to adopt effective policies in controlling sediment pollution of aquatic ecosystems that is becoming more and more pervasive.

## Materials and Methods

To understand the impact of watershed characteristics on watershed-scale sediment export, we incorporated hundreds of basins across CONUS into our analysis, which span climatological, geographical, and land use gradients. We retrieved 15-min high-frequency data of discharge, specific conductance, and turbidity for all USGS and NEON stations meeting our selection criteria. Our data search was constrained to include sites that were: 1) defined as “surface rivers and streams” and 2) had concurrent data for all three parameters for any period between 2000 and 2022. Storm events were extracted from the flow time series at each site by retrieving the rising and falling limb periods before and after flow exceeds the 90<sup>th</sup> percentile of site-specific streamflow. Short data gaps (<3 h) were filled using interpolation, whereas longer gaps were left in place. In addition to the high-frequency time series data, we acquired static watershed characteristics corresponding to each station using the USGS Geospatial Attributes of Gages for Evaluating Streamflow (GAGES II) (Falcone, 2011).

We performed hysteresis analysis to investigate event-based timing, sources, and pathways of sediment transport across CONUS. Sediment hysteresis is the asynchronous sediment-discharge relationship that is broadly classified into clockwise and counterclockwise patterns (Figure 1). Clockwise hysteresis occurs when sediment peaks before discharge, indicating proximal sourcing or rapid source mobilization. Conversely, in counterclockwise patterns, the peak of sediment occurs after discharge, suggesting distal sourcing of sediment or slow source mobilization (Lloyd et al., 2016). To quantitatively compare the hysteresis patterns, we employed two widely used metrics, namely the Hysteresis Index (HI) and the Flushing index (FI) that both vary between -1 and +1 (Lloyd et al., 2016; Vaughan et al., 2017). The sign of HI indicates clockwise (positive) or counterclockwise (negative) hysteresis, respectively, whereas the sign of FI suggests a flushing (positive) or diluting (negative) sediment storm response.

At any moment, discharge in a stream is principally comprised of two water components or pathways: baseflow and runoff (Figure 1). To understand how hydrologic pathways influence the arrival and magnitude sediment during an event, we developed a new index ( $\beta'_{runoff}$ ) that couples hydrograph separation with multiple linear regression of turbidity. Hydrograph separation was performed using specific conductance (SC) end-member mixing analysis (EMMA) that is governed by the following equations:

$$Q_{total} = Q_{Runoff} + Q_{baseflow}$$

$$Q_{total}SC_{total} = Q_{Runoff}SC_{runoff} + Q_{baseflow}SC_{baseflow}$$

Here,  $Q$  is the discharge,  $SC$  is the specific conductance value, and runoff and baseflow refer to the event water and the water that already exists in the watershed, respectively. To estimate  $SC_{runoff}$ , we used commonly used specific conductance values for rainfall and runoff in the literature (Hasenmueller et al., 2017, Cartwright and Miller, 2021), which typically range from 5 to 100 uS/cm and differ significantly from  $SC_{baseflow}$  values, which typically exceed 400 uS/cm in our study.  $SC_{baseflow}$  was estimated by taking the average  $SC$  value during the 48-hour period preceding event onset. To ensure the estimated  $SC_{baseflow}$  and  $SC_{runoff}$  accurately represent the baseflow and runoff conditions, we selected only the events where the  $SC$  at the start and peak of the event were greater than the 95th percentile and less than the 5th percentile (Miller et al., 2017), respectively, of the site-specific  $SC$  during the entire period. Solution of the above SC-EMMA system of equations provides continuous estimates of  $Q_{runoff}$  and  $Q_{baseflow}$ .

To infer the relative significance of  $Q_{runoff}$  and  $Q_{baseflow}$  to sediment generation during storm events, we employed multiple linear regression (MLR) with in-stream turbidity as the dependent variable, and  $Q_{runoff}$  and  $Q_{baseflow}$  as independent values for each storm event:

$$T_{total} = \beta_{runoff} Q_{runoff} + \beta_{baseflow} Q_{baseflow} + \epsilon$$

where  $T_{total}$  is the in-stream measured turbidity (NTU),  $Q_{runoff}$  and  $Q_{baseflow}$  are the estimated runoff and baseflow values,  $\beta_{runoff}$  and  $\beta_{baseflow}$  are coefficients associated to each independent variable, and  $\epsilon$  is the error term. We constrained  $\beta_{runoff}$  and  $\beta_{baseflow}$  to be non-negative and assumed their magnitude indicates the importance of their corresponding water component to sediment dynamics during the storm. To allow for cross-site and cross-storm comparison of the MLR coefficients, we introduced a new index  $\beta'_{runoff}$  by normalizing the runoff coefficient in the regression equation:

$$\beta'_{runoff} = \frac{\beta_{runoff}}{\beta_{runoff} + \beta_{baseflow}}$$

$\beta'_{runoff}$  varies between 0 and 1, where the extreme cases  $\beta'_{runoff} = 0$  and  $\beta'_{runoff} = 1$  indicate the turbidity signal is completely aligned with baseflow or runoff, respectively.

Finally, we conducted principal component analysis (PCA) to determine controls on hysteresis patterns and the contributions of runoff to stormflow and turbidity generation during the events. The explanatory variables include watershed properties (e.g., drainage area, impervious surface coverage), and climate variables (e.g., annual mean temperature and precipitation). Potential controls were defined as those that occupy the same dimensionally reduced space as the target variables ( $HI$ ,  $FI$ ,  $Q_r/Q$ ,  $\beta'_{runoff}$ ) on the PCA loading map.

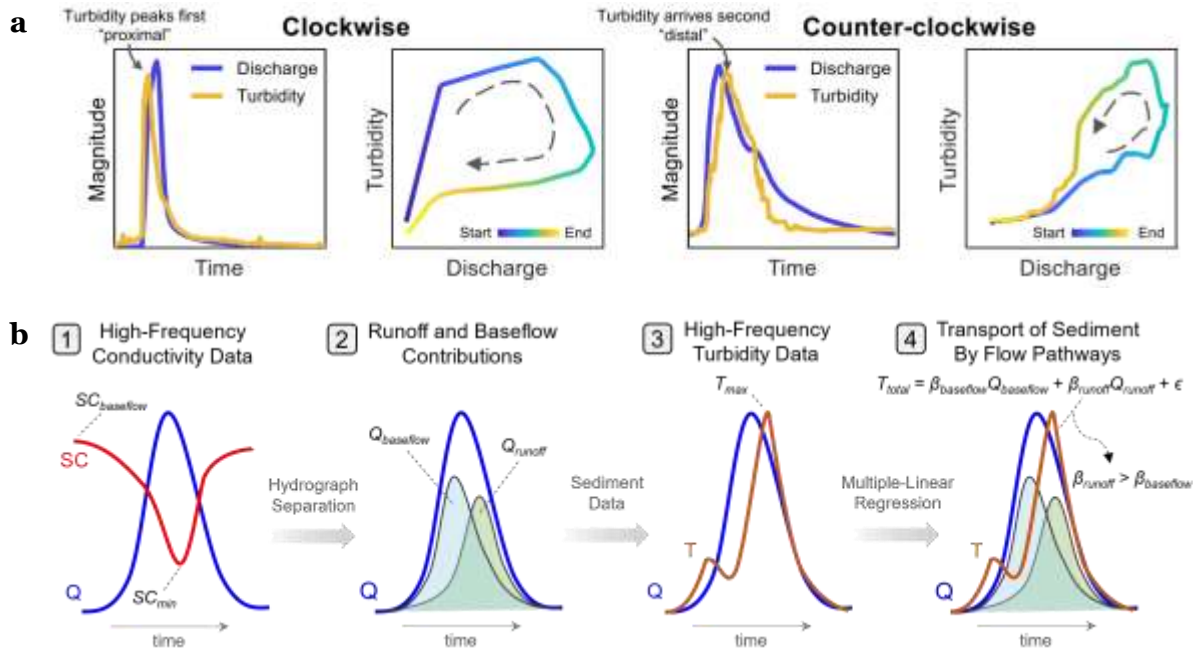


**Figure 1.** A conceptual figure of **a** sediment hysteresis patterns (adapted from Zarnaghsh and Husic, 2021) and **b** estimating the contribution of water components to turbidity generation

## Results

A total of 397 stations recorded at least a single storm event during the 22-year study period (2000 to 2022). Thereafter, stations with fewer than 10 storm events were excluded from further analysis as the small size of recorded events may not be representative of typical basin behavior. This left us with a total number of 38,036 storm events that were detected in 267 sites. We observed a positive  $HI$  in 73% of the sites (Figure 2). The percentage of sites with an average  $HI > 0.2$  or  $HI < -0.2$  were 28.1% and 1.9%, respectively, indicating that most sites have a relatively small magnitude of hysteresis. This result shows that the sediment and discharge peaks occur in close succession to one another in most watersheds. Regarding the flushing and dilution patterns, the average  $FI$  value for all sites was 0.60 and 16.9% of the sites had an average  $FI > 0.75$  indicating the prevalence of sediment flushing patterns across CONUS. While it is difficult to infer any spatial patterns in the variability of  $HI$  and  $FI$  (Figure 3), we generally observe lower average  $HI$  and  $FI$  in the sites located in the Northcentral and Midwest regions of the US.

Of the 38,036 events analyzed for turbidity analysis, 22,373 events, spanning 219 sites, met the criteria for hydrograph separation and MLR analysis. Hydrograph separation results showed that the baseflow is a larger contributor to overall streamflow in the vast majority (90.4%) of sites ( $Q_r/Q < 0.5$ ; Figure 2). While baseflow may generally composed a larger fraction of total streamflow, results of the new metric ( $\beta'_{runoff}$ ) show that runoff timing of arrival was more important to generating higher sediment concentrations than turbidity in 89% of sites. The mean  $\beta'_{runoff}$  was equal to 0.70, which exceeds the value at which baseflow and runoff equally contribute to the stream sediment signal ( $\beta'_{runoff} = 0.5$ ).

The studied sites were separated by basin climatological settings (Figure 4a). Temperate area sites were more urbanized with a higher proportion of flushing pattern events, while continental sites were less urbanized and less flashy. Hysteresis patterns were mainly climate-driven, but difficult to associate with a particular climatological group. Further, although  $Q_r$  and urban indicators shared the same space on the principal component plot, suggesting correlation,  $\beta'_{runoff}$  was not influenced by watershed characteristics (Figure 4b).

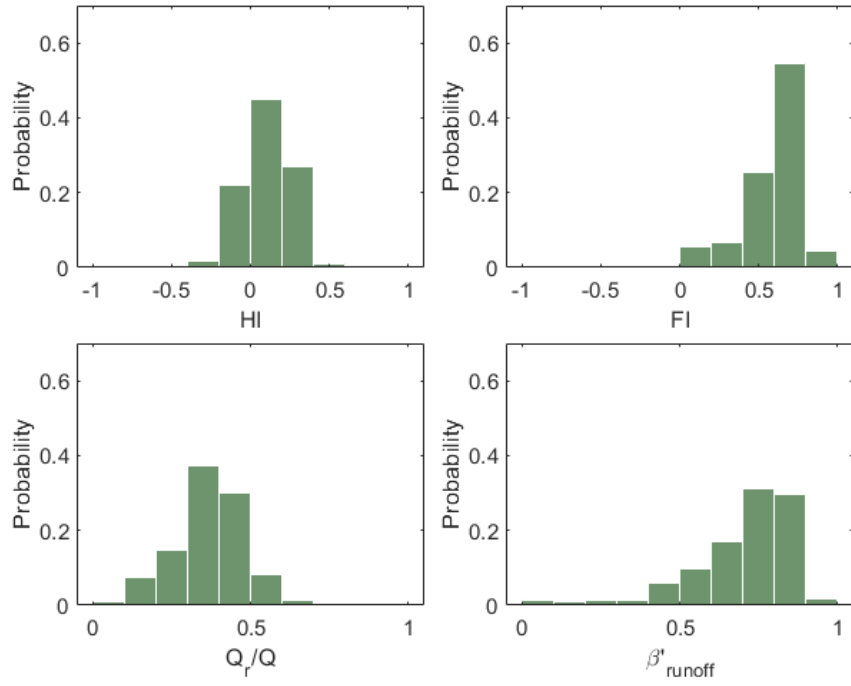


**Figure 2.** Histograms of  $HI$ ,  $FI$ ,  $Q_r/Q$ , and  $\beta'_{runoff}$

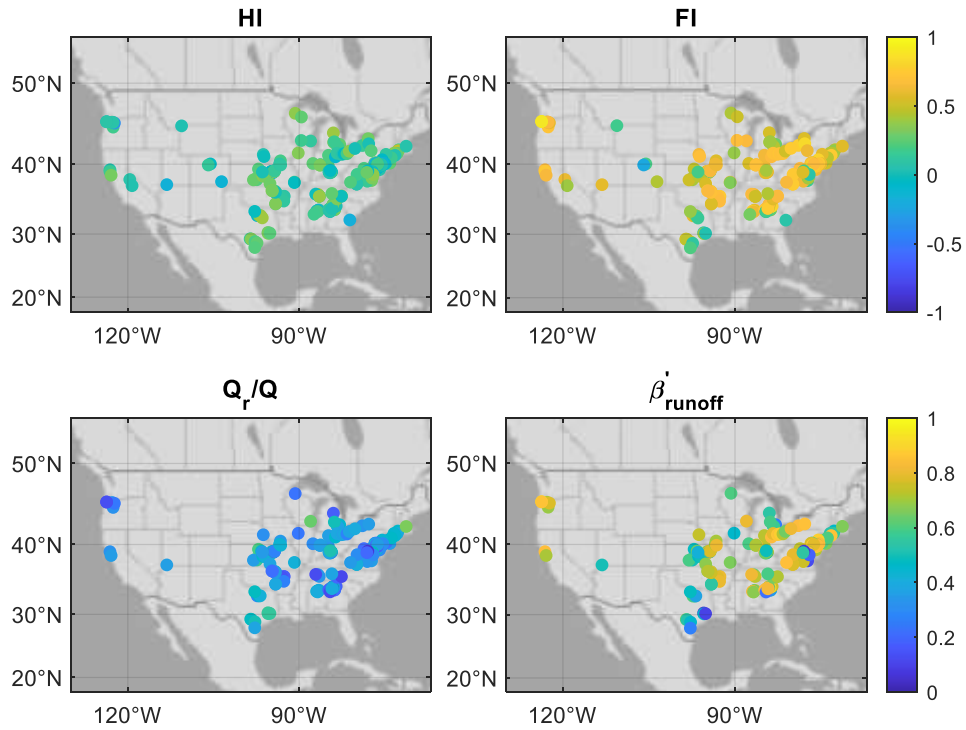


**Figure 3.** Spatial distribution of  $HI$ ,  $FI$ ,  $Q_r/Q$ , and  $\beta'_{runoff}$

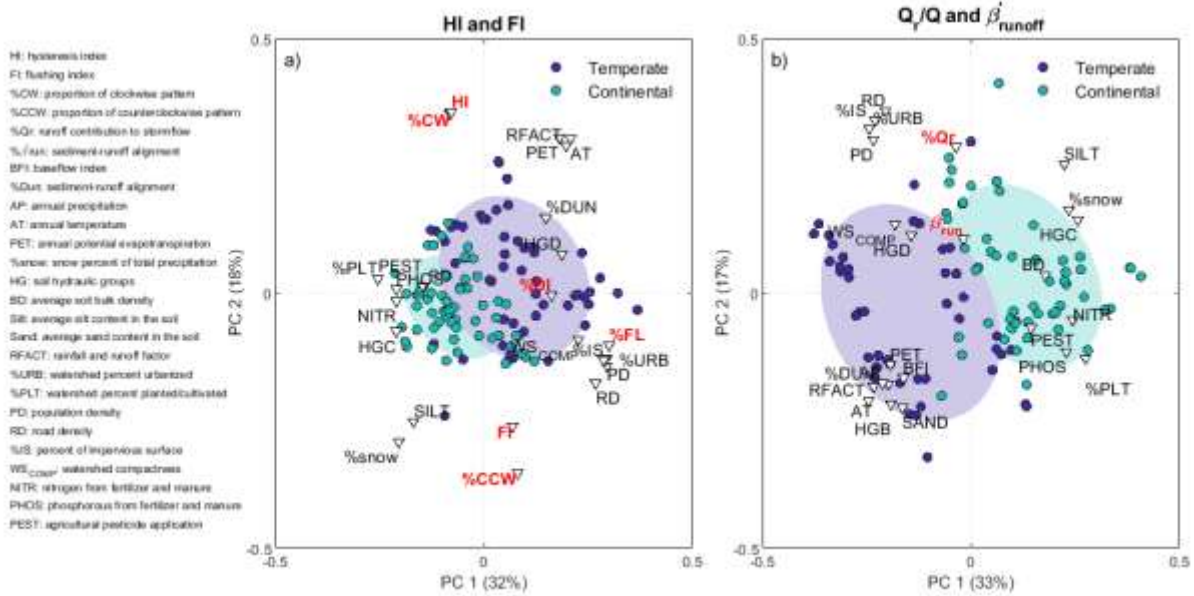


**Figure 4.** Principal Component Analysis (PCA) showing the relationship between watershed characteristics and a) hysteresis patterns ( $HI$  and  $FI$ ) and b) runoff contribution to storm events ( $Q_r/Q$ ) and alignment with sediment generation in streams ( $\beta'_{runoff}$ ).

### Discussion and Conclusion

Our hysteresis results indicate a high extent of sediment flushing during large storm events in the majority of CONUS basins. While the magnitude of  $HI$  was generally small, indicating similar timing of water and turbidity peaks during an event,  $HI$  was positive in about 70% of the events (turbidity peaks before discharge), suggesting the significance of proximal sediment sourcing or rapid sediment mobilization to basin-scale sediment export. Analyzing  $\beta'_{runoff}$  across CONUS, we found that although surface runoff typically constitutes a smaller fraction of stormflow compared to baseflow, it has a larger impact on the dynamics of sediment generation during storm events. The variability of flushing and diluting patterns is influenced by land-use characteristics as well as climate; however, further studies are required to fully untangle the relative impact of each of these factors. Together, these results provide new evidence for the possibility of coupling high-frequency sensor water quality data with hydrograph separation results to gain a better understanding of hydrology impacts on sediment mobilization to water bodies.

## References

- Vercruyse, K., Grabowski, R. C., & Rickson, R. J. (2017). Suspended sediment transport dynamics in rivers: Multi-scale drivers of temporal variation. *Earth-Science Reviews*, 166, 38-52.
- Oeurng, C., Sauvage, S., & Sánchez-Pérez, J. M. (2010). Dynamics of suspended sediment transport and yield in a large agricultural catchment, southwest France. *Earth Surface Processes and Landforms*, 35(11), 1289-1301.
- Ziegler, A. D., Benner, S. G., Tantasirin, C., Wood, S. H., Sutherland, R. A., Sidle, R. C., ... & Fox, J. M. (2014). Turbidity-based sediment monitoring in northern Thailand: Hysteresis, variability, and uncertainty. *Journal of Hydrology*, 519, 2020-2039.
- Mukundan, R., Pierson, D. C., Schneiderman, E. M., O'donnell, D. M., Pradhanang, S. M., Zion, M. S., & Matonse, A. H. (2013). Factors affecting storm event turbidity in a New York City water supply stream. *Catena*, 107, 80-88.
- Lloyd, C. E., Freer, J. E., Johnes, P. J., & Collins, A. L. (2016). Using hysteresis analysis of high-resolution water quality monitoring data, including uncertainty, to infer controls on nutrient and sediment transfer in catchments. *Science of the Total Environment*, 543, 388-404.
- Wymore, A. S., Leon, M. C., Shanley, J. B., & McDowell, W. H. (2019). Hysteretic response of solutes and turbidity at the event scale across forested tropical montane watersheds. *Frontiers in Earth Science*, 7, 126.
- Zarnaghsh, A., & Husic, A. (2021). Degree of anthropogenic land disturbance controls fluvial sediment hysteresis. *Environmental Science & Technology*, 55(20), 13737-13748.
- Hasenmueller, E. A., Criss, R. E., Winston, W. E., & Shaughnessy, A. R. (2017). Stream hydrology and geochemistry along a rural to urban land use gradient. *Applied Geochemistry*, 83, 136-149.
- Miller, M. P., Tesoriero, A. J., Hood, K., Terziotti, S., & Wolock, D. M. (2017). Estimating discharge and nonpoint source nitrate loading to streams from three end-member pathways using high-frequency water quality data. *Water Resources Research*, 53(12), 10201-10216.
- Falcone, J. A. (2011). *GAGES-II: Geospatial attributes of gages for evaluating streamflow*. US Geological Survey.
- Vaughan, M. C., Bowden, W. B., Shanley, J. B., Vermilyea, A., Sleeper, R., Gold, A. J., ... & Schroth, A. W. (2017). High-frequency dissolved organic carbon and nitrate measurements reveal differences in storm hysteresis and loading in relation to land cover and seasonality. *Water Resources Research*, 53(7), 5345-5363.
- Cartwright, I., & Miller, M. P. (2021). Temporal and spatial variations in river specific conductivity: Implications for understanding sources of river water and hydrograph separations. *Journal of Hydrology*, 593, 125895.